Predicting origami-inspired programmable self-folding of hydrogel trilayers

2016 Smart Mater. Struct. 25 11LT02

(http://iopscience.iop.org/0964-1726/25/11/11LT02)

Letters

IOP Publishing

Smart Materials and Structures

Smart Mater. Struct. **25** (2016) 11LT02 (8pp)

doi:10.1088/0964-1726/25/11/11LT02

Letter

Predicting origami-inspired programmable self-folding of hydrogel trilayers

Ning An[1], Meie Li[2] and Jinxiong Zhou[1]

[1] State Key Laboratory for Strength and Vibration of Mechanical Structures and School of Aerospace, Xi'an Jiaotong University, Xi'an 710049, People's Republic of China
[2] State Key Laboratory for Mechanical Behavior of Materials, School of Materials Science and Engineering, Xi'an Jiaotong University, Xi'an 710049, People's Republic of China

E-mail: limeie@mail.xjtu.edu.cn

Received 1 April 2016, revised 26 August 2016
Accepted for publication 1 September 2016
Published 18 October 2016

Abstract

Imitating origami principles in active or programmable materials opens the door for development of origami-inspired self-folding structures for not only aesthetic but also functional purposes. A variety of programmable materials enabled self-folding structures have been demonstrated across various fields and scales. These folding structures have finite thickness and the mechanical properties of the active materials dictate the folding process. Yet formalizing the use of origami rules for use in computer modeling has been challenging, owing to the zero-thickness theory and the exclusion of mechanical properties in current models. Here, we describe a physics-based finite element simulation scheme to predict programmable self-folding of temperature-sensitive hydrogel trilayers. Patterning crease and assigning mountain or valley folds are highlighted for complex origami such as folding of the Randlett's flapping bird and the crane. Our efforts enhance the understanding and facilitate the design of origami-inspired self-folding structures, broadening the realization and application of reconfigurable structures.

Keywords: origami, hydrogel, self-folding, finite element method, trilayer

(Some figures may appear in colour only in the online journal)

1. Introduction

Origami-an ancient art and science of paper folding-has long been the source of inspiration for reconfigurable and multifunctional materials and structures [1–10]. The fundamental principles of origami have been emulated and translated to achieve innovative devices and structures that have not only aesthetic but also functional characteristics, ranging across scales from nanoscale DNA folding [1, 2] to very large scale deployable aerospace structures such as solar sails and solar panels [11–14]. Other successful demonstrations of origami-inspired engineering include batteries [15], morphing wings [16], robotics [17–19], mechanical metamaterials [6–10], energy absorbers [20], and architectures [21].

More recently, there has been an upsurge of interests to develop origami-inspired self-folding structures, where transformations of folding shapes occur autonomously without external manipulations [3, 6, 8, 13, 14, 18, 19, 22]. The feature of self-folding is essential for some circumstances at very small or very large scales or in remote applications [23]. For microscale fabrication, delicate operations are needed to accurately execute the fabrication process; for very large space structures, external manipulations would increase the complexity of structure and risk of failure; for remote underwater robotics or invasive biological devices, external operation is impractical or prohibitive. One way to develop self-folding structures is to leverage the use of active or programmable materials whose properties can be predetermined to achieve desired configurations or stiffness on demand. Typical examples of using active materials to fabricate origami-inspired self-folding structures comprise shape memory alloy enabled programmable matter [6], reversible

self-folding sheets made of stimulus-responsive hydrogels or polymers [22, 24–26], and shape memory polymer-based self-folding machines [19].

Among various active materials for choices to fabricate origami-inspired self-folding structures, stimulus-responsive polymers or hydrogels have attracted considerable interests, owing to their fidelity of synthesis protocols, diversity of sensitivities to environmental stimuli, and sometimes the characteristics of wetness and softness that are excluded by traditional hard materials. One basic design of polymeric self-folding structures is a thin bimaterial sheet by laminating active polymer layers on inactive polymeric or metal films [27–29]. In response to changes of external environmental stimuli, the active polymer layers deform and mismatch strain is induced at the bimaterial interface, and the mismatch strain causes bending and folding of the sheet. Folding a planar polymeric bimaterial sheet into a 3D origami-inspired structure has been explored across various areas. On the biological or micromechanical front, for example, there have been successful demonstrations on micro-grippers [30], drug-vehicles [27, 29, 31], and batteries or electronics [15, 32], to mention just a few examples. This basic design of using bilayer sheets, nevertheless, can only achieve very simple origami structures, box being one of the examples frequently shown in literature [24, 29]. Very recently, this basic design using polymer bilayers evolves to a trilayer structure, where the active polymer is sandwiched between two inert stiff layers with patterned openings for mountain and valley folds assignment [22]. This trilayer structure design extends the feasibility of origami-inspired structures, and a complex Randlett's flapping bird origami has been demonstrated using a temperature-sensitive Poly(N-isopropl acrylamide-co-sodium acrylate) (PNIPAM) copolymer.

The core of origami-inspired engineering is the patterning of creases and assigning of mountain and valley folds, along with accurate deformation control of the constrained active materials. To successfully fabricate a complex microscale Randlett's bird-like origami structure, it is clear that development of origami modeling tools, if possible, would aid and ease the design of origami-inspired structures that are otherwise be carried out in a time-consuming trial-and-error manner. There has been a body of work in origami mathematics, algorithms, and even simulation software [33, 34]. These origami modeling tools, however, have two obvious limitations to predict self-folding of active polymers based origami structures [21, 23, 35, 36]: most of the origami algorithms assume zero-thickness of the folded structures, while the bilayer or trilayer structures concerned here have finite thickness; Another drawback of these approaches lies in the fact that they tend to exclude considerations on physical and mechanical properties of materials, which are crucial if we are to predict the mechanical response of origami structures and correlate it with prescribed external stimuli.

Here, we describe a physics-based modeling scheme that uses the powerfulness of the commercial finite element (FE) method, along with the rich sources of experimental data and thermodynamics models of temperature-sensitive hydrogels, in particular, PNIPAM hydrogels, that have been accumulated in literature. Each layer of the trilayer structure was discretized by three-dimensional (3D) solid elements, accommodating finite film thickness intrinsically; a thermodynamics model of PNIPAM hydrogel was adopted, accounting for nonlinear rubber elasticity, entropy and enthalpy of mixing polymers with solvents. We coded a user hyperelastic material subroutine, UHYPER, in ABAQUS, which enables us to design and program crease patterns and qualitatively predict the folded shapes and angles of complicated origami structures. Self-folding of miura-ori and Randlett's Flapping bird was imitated with qualitative agreement with reported experiment, and crease pattern for folding of a crane was designed and the folding process was predicted. We believe our efforts enhance the understanding of origami-inspired self-folding structures, and the approach enables design of crease patterns as well as high-fidelity prediction of origami-folding.

2. Theory and methodology

We follow the previously developed nonlinear field theory of coupled diffusion and deformation of polymer gels [37–39]. Introducing the first and the third invariants of the deformation gradient tensor $\mathbf{F}$, $I_1 = F_{iK}F_{iK}$ and $I_3 = \det \mathbf{F}$, respectively, and the nominal concentration of polymer molecules C, the Flory–Rehner type free energy for hydrogel is written as

$$W(I_1, I_3, C, T) = \frac{1}{2}Nk_BT(I_1 - 3 - 2\log I_3) - \frac{k_BT}{v}\left[vC\log\left(1 + \frac{1}{1+vC}\right) + \frac{\chi}{1+vC}\right], \quad (1)$$

where N is the number of chains per polymer volume, T is temperature, v is the volume of a solvent molecule, and k_B is the Boltzmann constant. A representative value of the volume per molecule is $v = 10^{-28}\,\mathrm{m}^3$. At room temperature, $k_BT = 4 \times 10^{-21}\,\mathrm{J}$. The first term in equation (1) represents the energy due to stretching of polymer network, and the two terms enclosed in the square bracket represent respectively the entropy and the enthalpy due to mixing of polymers with solvents. The Flory–Huggins interaction parameter, χ, measures the enthalpy of mixing of polymers and solvents, specifically, here we set χ to be 0.1.

In practice, it is more convenient to use displacement together with chemical potential μ as independent variables rather than the concentration C used in equation (1). Switching independent variable from C to μ via the Legendre transformation, and in addition, enforcing the condition of molecular incompressibility, $I_3 = 1 + Cv$, the free energy in

equation (1) is now converted to the following expression

$$\hat{W}(I_1, I_3, \mu, T) = \frac{1}{2}Nk_BT(I_1 - 3 - 2\log I_3) - \frac{k_BT}{v}\left[(I_3 - 1)\log\frac{I_3}{I_3 - 1} + \frac{\chi}{I_3}\right] - \frac{\mu}{v}(I_3 - 1). \quad (2)$$

With the free energy prescribed in equation (2), the derivatives of the free energy with respect to I_1 and I_3 are evaluated straightforwardly as

$$\frac{\partial W}{\partial I_1} = \frac{1}{2}Nk_BT, \quad (3)$$

$$\frac{\partial W}{\partial I_3} = -Nk_BT/I_3 - \frac{k_BT}{v}\left[\log\frac{I_3}{I_3 - 1} - \frac{1}{I_3} - \frac{\chi}{I_3^2}\right] - \frac{\mu}{v}. \quad (4)$$

The expression of stresses immediately follows and for example the first Piola–Kirchhoff stress, **P**, computed as

$$\mathbf{P} = \frac{\partial W_0(I_1, I_3)}{\partial \mathbf{F}} = \frac{\partial W_0(I_1, I_3)}{\partial I_1}\frac{\partial I_1}{\partial \mathbf{F}} + \frac{\partial W_0(I_1, I_3)}{\partial I_3}\frac{\partial I_3}{\partial \mathbf{F}}. \quad (5)$$

Other forms of stress tensors can also be obtained by using the stress relations. The ABAQUS UHYPER subroutine developed by Hong *et al* [40] is chosen here because it is pretty simple and only equations (3) and (4) are needed. For other user-subroutines, the explicit expressions of stresses and the tangent moduli are requisites for programming. In our simulations, in line with the strategy adopted by Wei *et al* [41], we adjust the solvent chemical potential to fit the volume phase transition of the copolymer.

The numerical simulations described in the following sections (sections 3 and 4) were conducted utilizing the commercial FE package, ABAQUS, version 6.14-4. The ABAQUS/Standard solver was employed for all the simulations and large deformation setting was turned on to capture the nonlinear large deformation. The temperature loading was enforced in an incremental manner, and static mechanical equilibrium was assumed in each increment without need to introduce damping. Each mesh comprises a large number of linear hybrid hexahedral elements (ABAQUS element type C3D8H) and a small number of linear hybrid wedge elements (ABAQUS element type C3D6H). More than 4 elements through the thickness of laminate layers were needed and a mesh refinement was also necessary along the folding creases, which would be shown in following section. The accuracy of each mesh was ascertained through a mesh refinement study.

3. Results and discussions

The hydrogel trilayer considered in this paper is fabricated by sandwiching a PNIPAM hydrogel membrane between two poly(*para*-methylstyrene) (PpMS) thin films. We start from a strip of a PpMS-PNIPAM-PpMS trilayer as shown in the inserted schematic in figure 1. A piece of temperature-sensitive PNIPAM hydrogel with thickness h_N is sandwiched between two layers of PpMS polymers, with one layer having an open width W and two layers have identical thickness h_p. As temperature drops, the hydrogel swells and the laminate folds, forming mountain in the region with open stripe while valley on the opposite side. In accordance with experiment reported in [22], the shear modulus of of hydrogel, identified as Nk_BT in equation (1), is taken as 0.267 MPa, and Young's modulus of PpMS is set to 4 GPa. In simulation, these parameters were normalized by k_BT/v and both were regarded as incompressible materials.

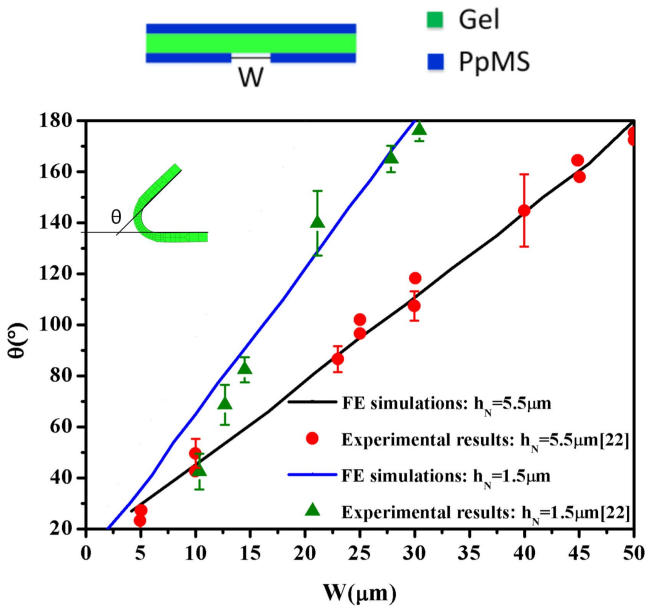

Figure 1. Comparison of folding angles of a hydrogel-trilayer versus open widths between FE simulations and experimental data reported in [22]. A piece of temperature-sensitive PNIPAM hydrogel is sandwiched between two layers of PpMS polymers, with one layer having an open width W. Two thicknesses of hydrogels, $h_N = 1.5\ \mu$m and 5.5 μm, as indicated in the legend, and a fixed thickness of PpMS layers $h_p = 70$ nm were considered in accordance with experiment. Variations of folding angles from 20° to 180° are achievable if open width varies from 5 to 50 μm and from 2 to 30 μm for a 5.5 μm and a 1.5 μm thick hydrogel, respectively.

We systematically probe the relationship between the folding angle θ and the width of opening set in one of the PpMS layers. Figure 1 plots the comparison of folding angles versus open widths between FE simulation and experimental data reported in reference [22]. In accordance with experiment, the thickness of PpMS layers is fixed as $h_p = 70$ nm and thickness of hydrogel is set to be $h_N = 1.5\ \mu$m and 5.5 μm as indicated in the legend of figure 1. For typical temperature modulation, say 55 °C–20 °C, variations of folding angles from 20° to 180° are achievable if open width varies from 5 to 50 μm and from 2 to 30 μm for a 5.5 and a 1.5 μm thick hydrogel, respectively. We only modeled the case that the opening was cut on the bottom PpMS layer, which is a valley fold. If otherwise the opening is cut on the top layer, it represents a mountain fold. The folding angles vary nearly linearly with the width of opening regardless

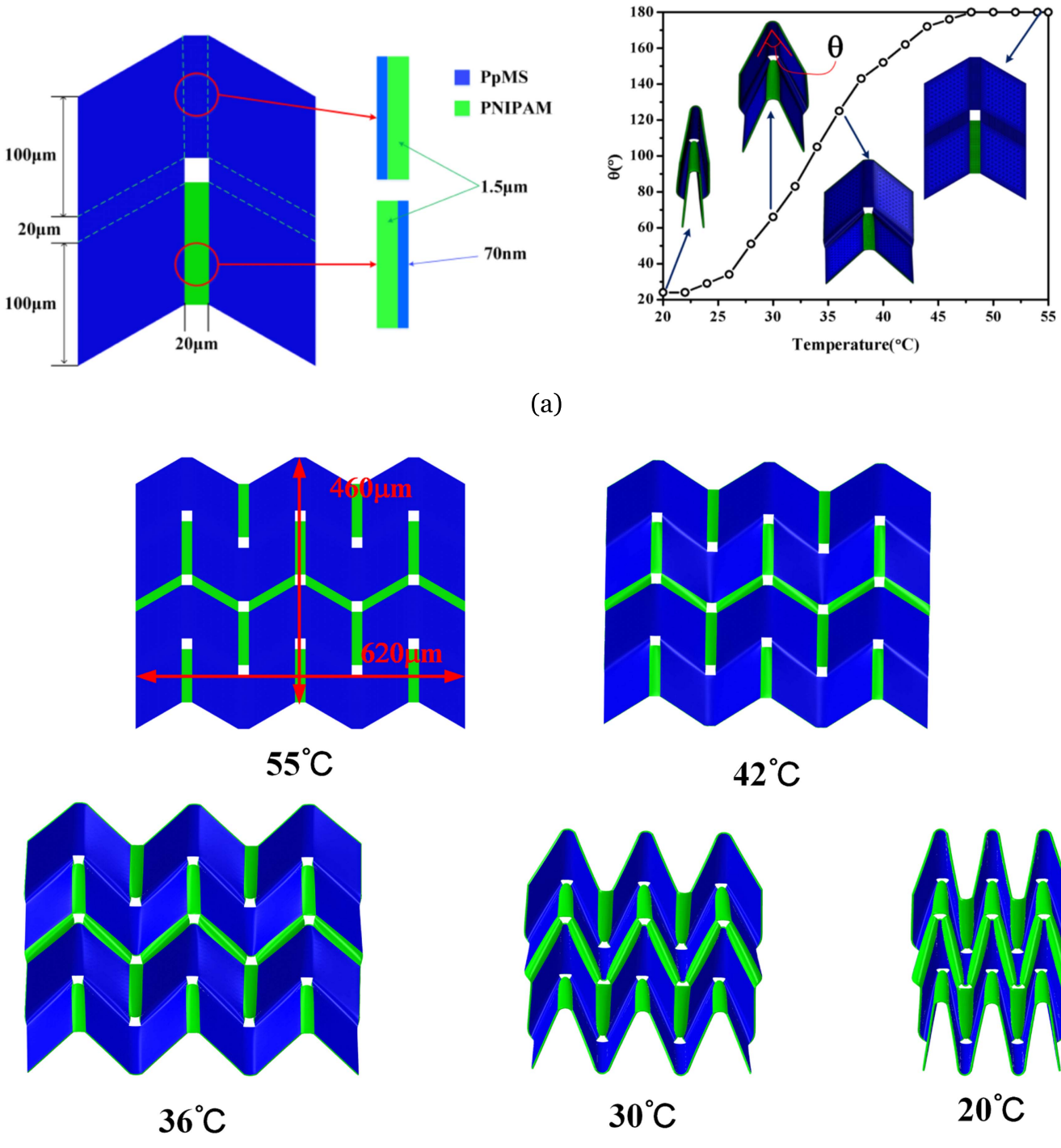

Figure 2. Predicted miura-ori self-folding. (a) Folding angles of a miura-ori unit cell versus temperature variation (right), along with the length scales and material distribution (left). (b) Self-folding process of a miura-ori structure comprising 6 unit cells. The opening widths are all set identically to 20 μm as indicated in (a). When the temperature is decreased from 55 °C to 20 °C, the swelling of PNIPAM causes the folding of the structure.

whether it is a mountain or valley fold. The linear folding angle versus opening width eases patterning of creases. The predicted liner relationship between folding angle and opening width as well as the range of variation are in good correlation with the experiment reported in [22]. However, there is a little discrepancy regarding the specific material constants used in simulation. For the hydrogel with larger thickness 5.5 μm, 0.267 MPa shear modulus given in [22] can give a good prediction, while for a thin 1.5 μm hydrogel the shear modulus is fitted to be 0.114 MPa. This discrepancy may arise from the data scatter of measurement of hydrogel materials especially when the hydrogel sheet is very thin. Because of lack of the details on the

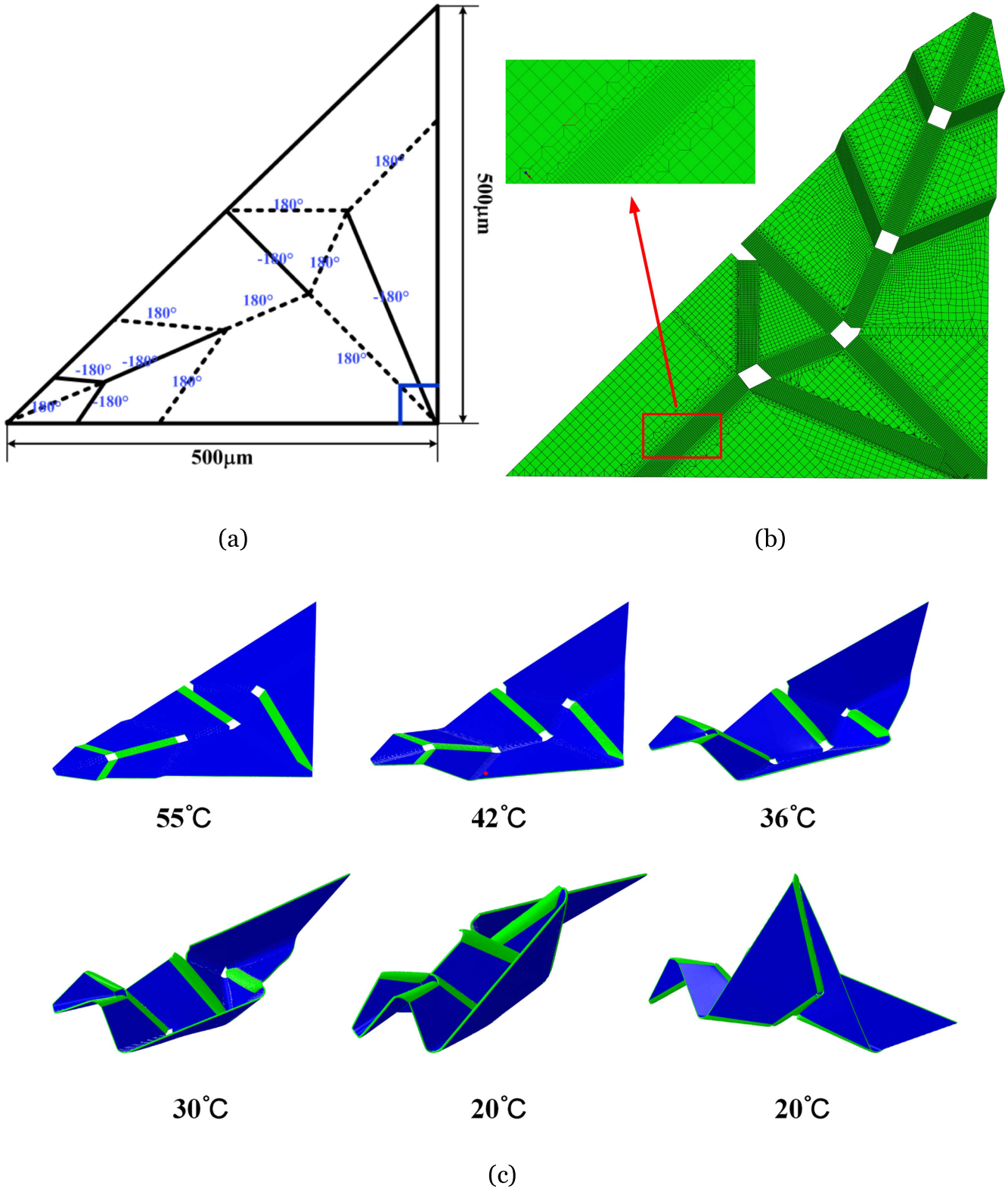

Figure 3. Self-folding of the Randlett's flapping bird. (a) The design of a trilayer film patterned to fold into a Randlett's bird. All open stripe widths are set to be 30 μm, such that all the foldings are 180°. The solid lines and the dashed lines represent the locations of mountain and valley folds, entailing controllable folding processes and programmable shape selections. (b) FE Mesh and detailed mesh transition. Mesh refinement is needed along the folding creases as shown by the manifested local view. (c) Folding configurations of the Randlett's bird as temperature varied from 55 °C to 20 °C, numerically reproducing the experiment reported in [22].

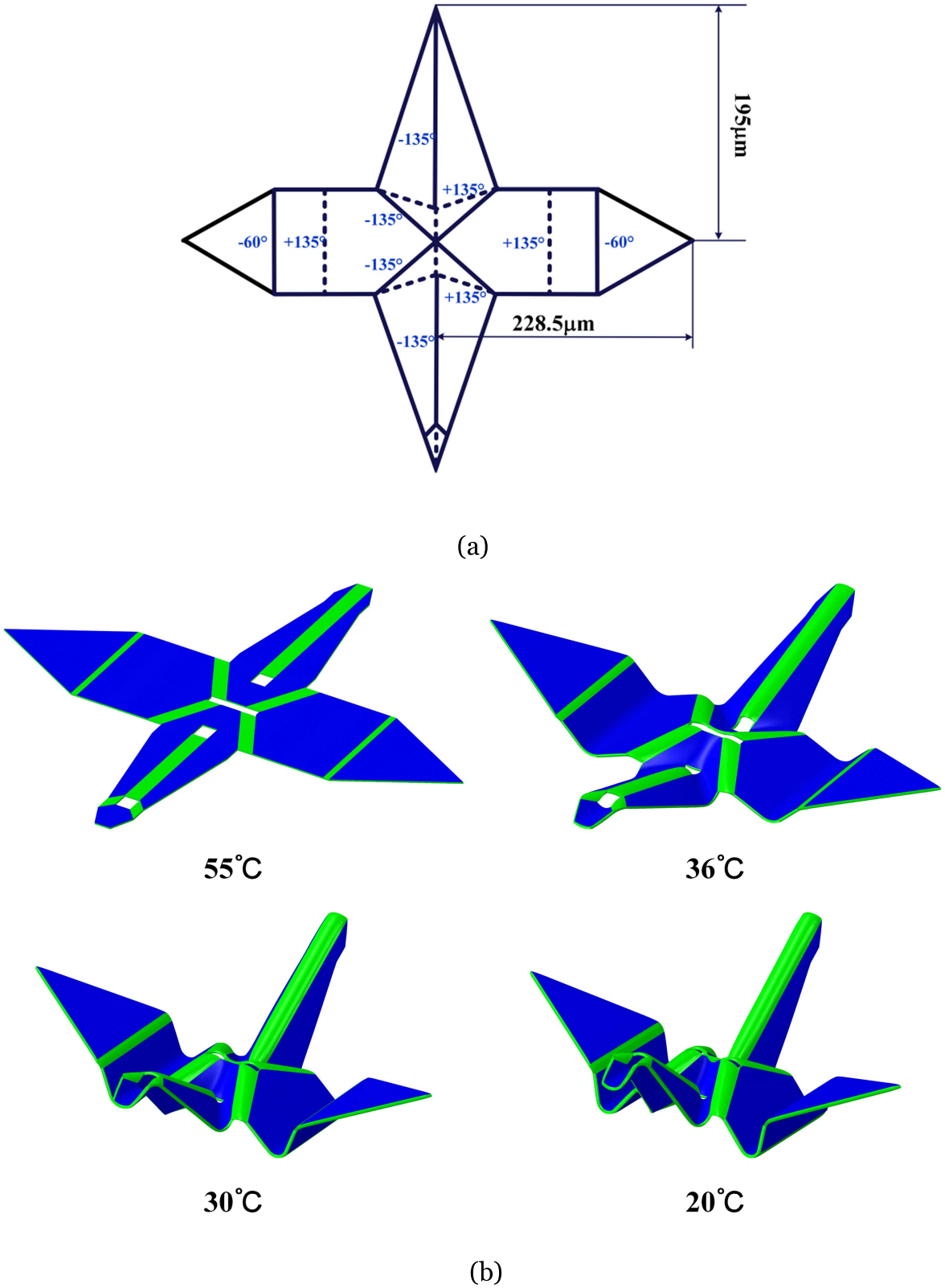

Figure 4. Predicted origami folding of the crane. (a) Pattern of the trilayer to fold a flat hydrogel sheet into a crane. (b) Predicted folding process of the crane as temperature varied from 55 °C to 20 °C.

mechanical parameters of the copolymer hydrogel, this discrepancy is understandable. Nevertheless, the whole story and the feasibility of the proposed strategy do not change.

Figure 1 actually gives the maximum possible folding angle that is achievable when temperature is varied within a realistic range, from 20 °C to 55 °C herein and in [22]. Given

a specific origami structure, the folded structure is determined by the crease pattern and the physical temperature variation. A reliable physical model should predict the dependence of folding angle on opening location, width, and more importantly on the specific variation of temperature. This was illustrated via a classic miura-ori origami given in figure 2. Figure 2(a) shows the crease pattern and material distribution of a unit cell of a miura-ori origami and the folding angle versus temperature curve. Figure 2(b) shows the origami process of a miura-ori structure comprising 6 unit cells. The dimensions of each unit cells are the same as that given in [22], we demonstrate here, by virtue of periodicity, the folding of a miura-ori structure with 6 units rather than 9 units in [22] to reduce computation cost. At vertices where creases intersect, a small cut was made and the fraction of material was removed from simulation. This avoids the stress singularity at the vertices and guarantees the smooth going of simulation. Note that when the temperature is 55 °C, the folding angle is 180°, corresponding to a flat state in figure 2(b); when the temperature is dropped to 20 °C, the PNIPAM at the opening swells and the structure folds into a compact state with folding angle approximately 20° as indicated by the last snapshot in figure 2(b). For intermediate temperatures, the model predicts the folding shapes that qualitatively agree well with experiment in [22]. It should be pointed that the bilayer structure at the opening works as a hinge, and the neighboring trilayer panels rotate rigidly as the hinge bends. This is the underlying working mechanism of such a hydrogel trilayer self-folding structures.

We then move in on the folding of Randlett's flapping bird. Because of symmetry of the structure, we only modeled half the self-folding structure for the purpose of computation saving. Figure 3(a) gives the design of crease pattern on a right triangle trilayer. All open stripe widths are set such that all the foldings are 180°. The solid lines and the dashed lines represent the locations of mountain and valley folds, respectively. Figure 3(b) demonstrates the FE Mesh and detailed mesh transition. Figure 3(c) presents the folding configurations of the Randlett's bird as temperature varied from 55 °C to 20 °C, qualitatively imitating the experiment reported in [22].

The physics-based model combined with the powerfulness of commercial FE software allows us to design and predict more complex origami-inspired self-folding structures. We finally show an example by folding a crane as shown in figure 4. This self-folding structure was previously implemented by Wood *et al* [42] by using shape memory polymers. Here we demonstrate that this specific origami folding can also be realized via a hydrogel trilayer construction. What a little difference from the miura-ori and the Randlett's bird foldings is that the involved folding angles and the opening widths are not the same in crane folding, while for the two previous examples all the foldings are 180° and thus openings for all mountain and valley folds are the same. Figure 4(a) presents the design of crease pattern with corresponding folding angles indicated at each crease, the associated opening widths being determined from the relation given in figure 1. Figure 4(b) demonstrates the folding process of the crane as temperature varies from 55 °C to 20 °C.

4. Concluding remarks

The art and science of origami has evolved from aesthetic pursuits to design folding structures across cultures and scales. Leveraging origami principles allow engineers to fabricate, assembly, store, and morph structures only through bending without any cutting and gluing. The resultant origami-inspired structures are featured by the capabilities of compact stowing, reconfigurability, and reduction in manufacturing complexity. When the origami principles are translated to soft active or programmable materials, which are characterized by their remarkable ability to respond to external stimuli in a variety of ways, the synergy of the two merits opens up fresh avenues for the development of origami-inspired self-folding structures. As one of the successful examples, hydrogels, a class of soft active materials, have been explored to achieve a substantial number of self-folding structures in either a bilayer or a trilayer fashion.

However, a generalized understanding of origami remains elusive, owing to the gap between experiment and the model prediction. The discrepancy arises from the drawback of the zero-thickness assumption and the limitation of precluding consideration of mechanical properties for the majority of current models. Here, we describe a physics-based FE simulation strategy which circumvents these two limitations, in the sense that the whole structure is discretized by 3D element thus accommodates finite thickness, and moreover, the mechanics and chemistry of a temperature-sensitive PNIPAM hydrogel are reflected as input parameters. Self-folding of miura-ori, Randlett's flapping bird, and a crane are successfully modeled with qualitative agreement with experiment reported in literature. The design of crease patterns as well as mountain and valley folds assignment are highlighted for qualitative prediction and correlation of model prediction with physical variation of external stimuli, e.g., temperature in this paper. We identify key factors such as crease pattern design, material constant contrast and geometric dimensions that govern self-folding process. Our efforts would aid the design, fabrication, and manipulation of origami-inspired self-folding structures. Prediction of programmable self-folding of more complicated origami structures and the validation of the prediction via experiment are expected.

Acknowledgments

This research is supported by Natural Science Foundation of China (grants 11372239, 11472210 and 11321062). We also thank Prof Ryan C Hayward for valuable discussions and providing crease pattern of Randlett's flapping bird model.

References

[1] Rothemund P W K 2006 Folding DNA to create nanoscale shapes and patterns *Nature* **440** 297–302
[2] Han D, Pal S, Nangreave J, Deng Z, Liu Y and Yan H 2011 DNA origami with complex curvatures in three-dimensional space *Science* **332** 342–6
[3] Py C, Reverdy P, Doppler L, Bico J, Roman B and Baroud C N 2007 Capillary origami: spontaneous wrapping of a droplet with an elastic sheet *Phys. Rev. Lett.* **98** 156103
[4] Ebbesen T W and Hiura H 1995 Graphene in 3-dimensions: towards graphite origami *Adv. Mater.* **7** 582–6
[5] Blees M K, Barnard A W, Rose P A, Roberts S P, McGill K L, Huang P Y, Ruyack A R, Kevek J W, Kobrin B and Muller D A 2015 Graphene kirigami *Nature* **525** 204–7
[6] Hawkes E, An B, Benbernou N, Tanaka H, Kim S, Demaine E, Rus D and Wood R 2010 Programmable matter by folding *Proc. Natl Acad. Sci.* **107** 12441–5
[7] Schenk M and Guest S D 2013 Geometry of Miura-folded metamaterials *Proc. Natl Acad. Sci.* **110** 3276–81
[8] Silverberg J L, Evans A A, McLeod L, Hayward R C, Hull T, Santangelo C D and Cohen I 2014 Using origami design principles to fold reprogrammable mechanical metamaterials *Science* **345** 647–50
[9] Lv C, Krishnaraju D, Konjevod G, Yu H and Jiang H 2014 Origami based mechanical metamaterials *Sci. Rep.* **4** 5979
[10] Silverberg J L, Na J-H, Evans A A, Liu B, Hull T C, Santangelo C D, Lang R J, Hayward R C and Cohen I 2015 Origami structures with a critical transition to bistability arising from hidden degrees of freedom *Nat. Mater.* **14** 389–93
[11] Zirbel S A, Lang R J, Thomson M W, Sigel D A, Walkemeyer P E, Trease B P, Magleby S P and Howell L L 2013 Accommodating thickness in origami-based deployable arrays *J. Mech. Des.* **135** 111005
[12] Courtland R 2010 Origami solar sail set to fly *New Sci.* **206** 10
[13] Liyanage P and Mallikarachchi H 2013 Origami based folding patterns for compact deployable structures *4th Int. Conf. for Structural Engineering and Construction Management* (doi:10.13140/2.1.4139.0082)
[14] Nishiyama Y 2012 Miura folding: applying origami to space exploration *Int. J. Pure Appl. Math.* **79** 269–79
[15] Song Z, Ma T, Tang R, Cheng Q, Wang X, Krishnaraju D, Panat R, Chan C K, Yu H and Jiang H 2014 Origami lithium-ion batteries *Nat. Commun.* **5** 3140
[16] Saito K, Agnese F and Scarpa F 2011 A cellular kirigami morphing wingbox concept *J. Intell. Mater. Syst. Struct.* **22** 935–44
[17] Dai J and Caldwell D 2010 Origami-based robotic paper-and-board packaging for food industry *Trends Food Sci. Technol.* **21** 153–7
[18] Onal C D, Wood R J and Rus D 2011 In towards printable robotics: origami-inspired planar fabrication of three-dimensional mechanisms *2011 IEEE Int. Conf. on Robotics and Automation (ICRA)* (Piscataway, NJ: IEEE) pp 4608–13
[19] Felton S, Tolley M, Demaine E, Rus D and Wood R 2014 A method for building self-folding machines *Science* **345** 644–6
[20] Ma J and You Z 2014 Energy absorption of thin-walled square tubes with a prefolded origami pattern: I. Geometry and numerical simulation *J. Appl. Mech.* **81** 011003
[21] Reis P M, Jiménez F L and Marthelot J 2015 Transforming architectures inspired by origami *Proc. Natl Acad. Sci.* **112** 12234–5
[22] Na J H, Evans A A, Bae J, Chiappelli M C, Santangelo C D, Lang R J, Hull T C and Hayward R C 2015 Programming reversibly self-folding origami with micropatterned photo-crosslinkable polymer trilayers *Adv. Mater.* **27** 79–85
[23] Peraza-Hernandez E A, Hartl D J, Malak R J Jr and Lagoudas D C 2014 Origami-inspired active structures: a synthesis and review *Smart Mater. Struct.* **23** 094001
[24] Guo W, Li M and Zhou J 2013 Modeling programmable deformation of self-folding all-polymer structures with temperature-sensitive hydrogels *Smart Mater. Struct.* **22** 115028
[25] An N, Li M and Zhou J 2015 Instability of liquid crystal elastomers *Smart Mater. Struct.* **25** 015016
[26] Gladman A S, Matsumoto E A, Nuzzo R G, Mahadevan L and Lewis J A 2016 Biomimetic 4D printing *Nat. Mater.* **15** 413–8
[27] Li X and Serpe M J 2014 Understanding and controlling the self-folding behavior of poly (N-Isopropylacrylamide) microgel-based devices *Adv. Funct. Mater.* **24** 4119–26
[28] Stoychev G, Turcaud S, Dunlop J W and Ionov L 2013 Hierarchical multi-step folding of polymer bilayers *Adv. Funct. Mater.* **23** 2295–300
[29] Ionov L 2011 Soft microorigami: self-folding polymer films *Soft Matter* **7** 6786–91
[30] Zheng W J, An N, Yang J H, Zhou J and Chen Y M 2015 Tough Al-alginate/Poly (N-isopropylacrylamide) Hydrogel with tunable LCST for soft robotics *ACS Appl. Mater. Interfaces* **7** 1758–64
[31] Lee D-Y, Kim J-S, Kim S-R, Koh J-S and Cho K-J 2013 In the deformable wheel robot using magic-ball origami structure *ASME 2013 Int. Design Engineering Technical Conf. and Computers and Information in Engineering Conf.* (American Society of Mechanical Engineers) p V06BT07A040
[32] Miyashita S, Meeker L, Tolley M T, Wood R J and Rus D 2014 Self-folding miniature elastic electric devices *Smart Mater. Struct.* **23** 094005
[33] Lang R J 1996 In a computational algorithm for origami design *Proc. 12th Annual Symp. on Computational Geometry* (New York: ACM) pp 98–105
[34] Tachi T 2010 In geometric considerations for the design of rigid origami structures *Proc. Int. Association for Shell and Spatial Structures (IASS) Symp.* pp 458–60
[35] Al-Mulla T and Buehler M J 2015 Origami: folding creases through bending *Nat. Mater.* **14** 366–8
[36] Chen Y, Peng R and You Z 2015 Origami of thick panels *Science* **349** 396–400
[37] Hong W, Zhao X, Zhou J and Suo Z 2008 A theory of coupled diffusion and large deformation in polymeric gels *J. Mech. Phys. Solids* **56** 1779–93
[38] Cai S and Suo Z 2011 Mechanics and chemical thermodynamics of phase transition in temperature-sensitive hydrogels *J. Mech. Phys. Solids* **59** 2259–78
[39] Zhou J, Hong W, Zhao X, Zhang Z and Suo Z 2008 Propagation of instability in dielectric elastomers *Int. J. Solids Struct.* **45** 3739–50
[40] Hong W, Liu Z and Suo Z 2009 Inhomogeneous swelling of a gel in equilibrium with a solvent and mechanical load *Int. J. Solids Struct.* **46** 3282–9
[41] Wei Z, Jia Z, Athas J, Wang C, Raghavan S R, Li T and Nie Z 2014 Hybrid hydrogel sheets that undergo pre-programmed shape transformations *Soft Matter* **10** 8157–62
[42] Felton S M, Tolley M T, Shin B, Onal C D, Demaine E D, Rus D and Wood R J 2013 Self-folding with shape memory composites *Soft Matter* **9** 7688–94